Electronic Supplementary Material (ESI) for Inorganic Chemistry Frontiers.
This journal is © the Partner Organisations 2020

Supporting Information

Stephanie M. Laga,[a] Tanya M. Townsend,[a,b] Abby R. O'Connor,[b] and James M. Mayer* [a]

[a] Department of Chemistry, Yale University, New Haven, CT 06520-8107, USA
[b] Department of Chemistry, The College of New Jersey, Ewing, NJ 08628, USA

1 General considerations 2
- 1.1 General Instrumentation 2
- 1.2 X-ray absorption spectroscopy 2
- 1.4 Preparation of cerium oxide for UV-visible spectroscopy with the OLIS CLARiTY 4
- 1.5 Chemicals 5

2 Nanoparticle systems 5
- 2.1 Cerium oxide nanoparticle preparation 5
- 2.2 Calculation of cerium concentration and the number of Ce atoms per particle 6
- Figure SI-1. TEM and XRD of cerium oxide systems. 7

3 Catalyst considerations 8
- 3.1 Preparation of Ir and Ru catalysts 8
- Figure SI-2. UV-visible spectra for [Ru] and [RuH_2] 8

4 Experiments with colloidal ceria and [RuH_2] 9
- Figure SI-3. Heating controls of [RuH_2] or oley-Ce NPs. 9
- Figure SI-4. ^{1}H NMR of oley-Ce and [RuH_2]. 10
- Figure SI-5. No effect of oleylamine capping ligand on [RuH_2]. 11
- Figure SI-6. Effect of oleate capping ligand on [Ru] and [RuH_2]. 12
- 4.1 Comments on the compatibility of capping ligands and homogeneous catalysts 12

5 ^{1}H NMR reactivity of uc-Ce and [RuH_2] 13
- Figure SI-7. ^{1}H NMR of uc-Ce and [RuH_2]. 13

6 Alcohol oxidation experiments 14
- 6.1 Screening of [Ir-SO_2(R)] catalysts for alcohol oxidation 14
- Figure SI-8. XAS of uc-Ce reduced by various [Ir-SO2(R)] catalysts 14
- Figure SI-8. Heating of [Ir-SO_2(Me)] and uc-Ce. 15
- 6.2 Experimental for catalytic alcohol oxidation reactions 16
- Figure SI-9. Adsorption of acetone to uncapped cerium oxide. 17
- Figure SI-10. Aerobic oxidation of substrates. 18

7 Reaction of cerium oxide and dihydroanthracene 19
Figure SI-11. Reaction of uncapped cerium oxide with dihydroanthracene. 19
8 Analysis of the size of cerium oxide post-reaction 20
Figure SI-12. Post-reaction XRD spectra of uncapped cerium oxide. 21
Figure SI-13. Post reaction TEM spectra of uncapped cerium oxide. 22
9 References 23

1 General considerations

1.1 General Instrumentation

UV-Vis spectra of organically capped cerium nanoparticles were recorded in an N_2-filled glovebox using an Agilent Cary 5000 spectrometer or in air on a Hewlett Packard 8453 diode array spectrophotometer, using 1 cm quartz cuvettes. Spectra of the cerium oxide nanopowder were collected using an Olis CLARiTY CCD spectrometer, using 1 cm diameter quartz tubes.

Powder X-ray diffraction (PXRD) patterns were obtained on a Rigaku MiniFlex600 Powder X-Ray Diffractometer with a sealed Cu-anode tube ($\lambda = 0.154$ nm) as the X-ray source.

^{1}H NMR spectra were collected on A500a Agilent DD2 500 MHz spectrometer and data were processed using MestReNova©. Chemical shifts were reported relative to TMS by referencing the residual solvent. All spectra are reported in deuterated toluene and were quantified relative to the internal standard 1,3,5-trimethoxybenzene (TMB).

TEM images were obtained on FEI Tecnai Osiris 200kV transmission electron microscope operating at 200kV. 5 µL of a 1mM nanoceria solution in cyclohexane was deposited on a lacey carbon 400 mesh Cu grid (Ted Pella, Inc.). The size and the distribution of NPs were obtained by counting >300 nanocrystalline particles using ImageJ software.

Inductively-coupled plasma mass spectroscopy (ICP-MS) was carried out using a Perkin Elmer ICP-MS Elan DRC-e instrument with Fluka TraceCERT® High Purity brand Ce standard (1000 µg/L in 2% HCl).

1.2 X-ray absorption spectroscopy

Fluorescence X-ray absorbance measurements at the Ce L_{III}-edge (5723 eV) were acquired at sector 20-BM-B (part of the X-ray Sciences Division) at the Advanced Photon Source, Argonne, IL.[4,5] Photon energies were selected using a fixed-exit double-crystal monochromator utilizing Si(111), which was detuned approximately 50% to reduce harmonic reflections. Cr (5989.02 eV) or V (5463.75 eV) pure foils[6] were run concurrently with experimental Ce samples and used for energy calibration. The incident (I_0), transmission (I_t), and reference (I_{ref}) detectors were ionization chambers using 70% He / 30% N_2 (I_0), and 90% N_2 / 10% Ar (I_t, I_{ref}). Fluorescence signals were collected using a 12 element Canberra Ge detector at 20-BM-B.

Transmission and Fluorescence data were acquired in parallel with a beam size of 800 × 1000 µm, using 3 separate regions (energies relative to the Ce elemental edge): a pre-edge region (-150 (-250 for samples using V reference foil) to -20 eV, 5 eV steps, integration time = 2 s), the XANES region (-20 to 30 eV, 0.3 eV steps, integration time = 2 s); and the EXAFS region (30 to 419.20 eV (10.49 k), 0.05 $Å^{-1}$ steps, integration time = 2 s with an additional k weighting of 1). The detector settling time was 0.1 s prior to each measurement with a beam size of 1.2 mm × 0.5 mm, and each scan took approximately 7 min. Signals from each channel of the fluorescence detector were summed for each scan, and at least three scans were taken per sample and averaged. All spectra were taken at room temperature.

All sample manipulations were performed in an inert atmosphere glovebox, unless noted otherwise. Spectra were calibrated to the Cr or V foil references and normalized using standard procedures in Athena.[7] Edge positions were determined by locating the maximum of the first peak in the first derivative spectrum. The ratio of cerium oxidation states was determined using Athena by fitting the XANES region (-15 to +30 eV) with an arctan and four unit normalized Gaussian functions as described in the results section. Transitions were identified from the literature.[1,2] The fits were performed with unit normalized Gaussians (meaning that the area and height are equivalent) using the software Athena[7] over the range of -15 to +30 eV (below).

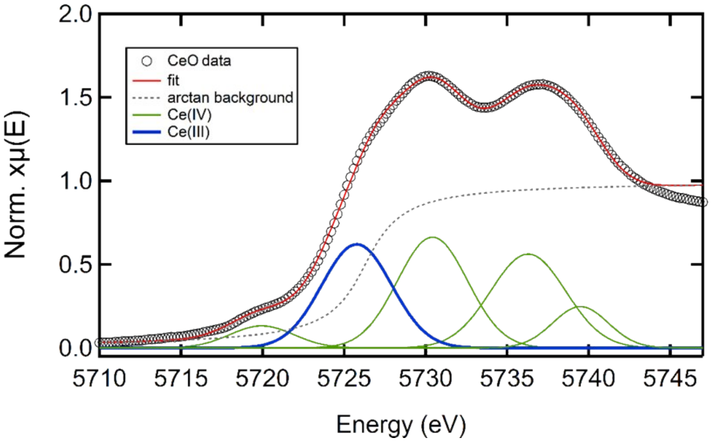

1.4 Preparation of cerium oxide for UV-visible spectroscopy with the OLIS CLARiTY

To prepare solid, uc-Ce for measurement using the OLIS CLARiTY,[3] it was first separated from the reaction suspension and treated according to the scheme shown below. Briefly, the separated solid is washed with clean solvent in an air-free environment to remove residual catalyst or substrate. The suspension is centrifuged and the washings decanted off. This process is repeated until the solution is no longer colored by the catalyst, about 3-4 times. The cleaned, uc-Ce is resuspended in either EtOH or THF in an air-free, quartz tube for measurement. After a CLARiTY spectrum of the reacted ceria is collected, the sample is exposed to air and allowed to stir for about 30 minutes to 1 hour. A follow-up spectrum is collected to confirm oxidation of the reacted ceria.

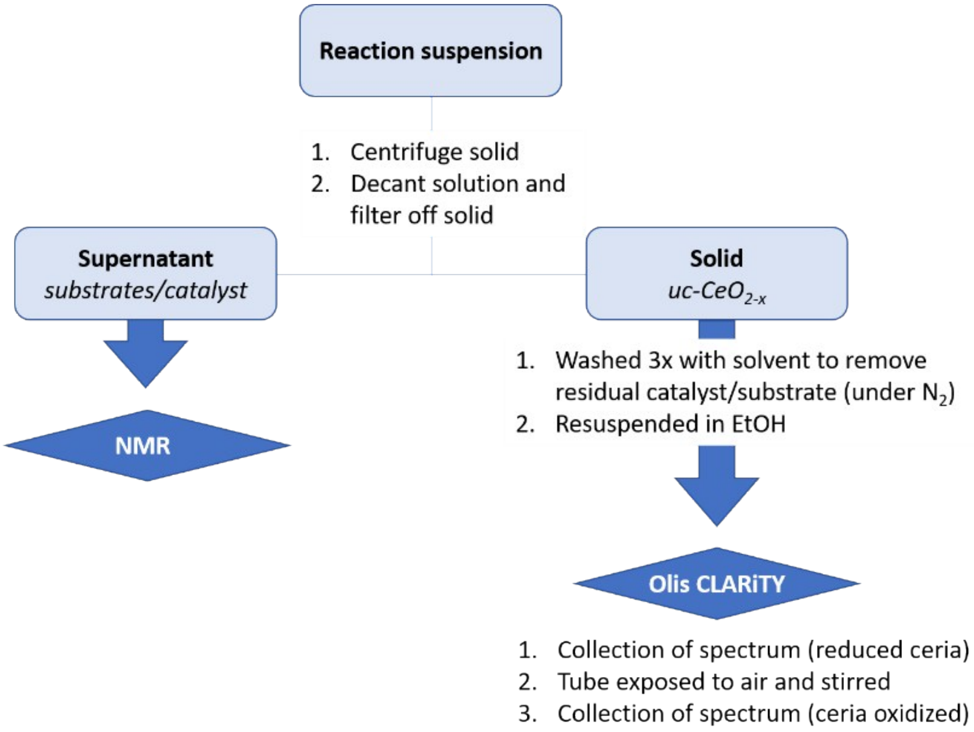

This procedure was developed because the CLARiTY is very sensitive to changes in concentration, and it allows measurement on the same sample tube without significant changes to the concentration of ceria in solution.

1.5 Chemicals

All chemicals were purchased commercially and used without further purification, unless noted otherwise. Deuterated solvents were purchased from Cambridge Isotopes Laboratories, Inc., degassed, and dried over activated 3 Å molecular sieves for 3 days. All other solvents were purchased from Fischer Scientific and were dried using a Seca Solvent System installed by Glass Contour.

2 Nanoparticle systems

2.1 Cerium oxide nanoparticle preparation

Oleate-capped ceria NPs were synthesyzed following a published procedure with minor modifications.[4] Sodium oleate ($C_{17}H_{33}COONa$, STREM, 99%, 1.06 g, 3.5 mmol) was dissolved in 15 mL of warm double distilled water (DDW), then cooled to room temperature and added dropwise to a stirring solution of 1.92 g (3.5 mmol) ammonium cerium nitrate ($(NH_4)_2Ce(NO_3)_6$, Sigma Aldrich, 99.9%) in 15 mL DDW. Subsequently, 4.5 mL of aqueous ammonia solution (28 wt%, Sigma Aldrich) was added dropwise under vigorous stirring to the reaction mixture. After 30 minutes of stirring, the crystalline products were collected by centrifugation (6500 rpm for 15 min), followed by decantation, and washed twice with distilled water to remove excess starting materials. After the last centrifugation and decantation, pale-brown solid materials were placed in a glass vial and dried at 90 °C for 24 h in tube furnace under air. The resulting brown solid was brought into an N_2 glovebox, and dissolved in cyclohexane, although some small amount of precipitate remained. These precipitates were removed by centrifugation at 6500 rpm for 10 min. Then, clear brown solution was stored under N_2 in the freezer (-35 ^oC).

Oleylamine-capped ceria NPs were synthesized following a published procedure.[5] Cerium nitrate hexahydrate (1.7g, 4mmol) was added to oleylamine (technical grade, 20 m: 16.26 g, 60 mmol) at room temperature. The mixture was heated to 90 °C under vacuum, causing the solution to turn brownish black. Following the addition of diphenyl ether (1 mL) under vacuum, the solution was heated for two hours at 320 °C under stream of N_2. Ethanol (50 mL) was used to precipitate the nanocrystals, which were collected by centrifugation. The light brown solid was redissolved in toluene, precipitated again with ethanol, and then centrifuged. The washed particles were finally brought into an N_2 glovebox, and dissolved in toluene, and stored under N_2 in a freezer (-35 ^oC).

The uncapped powder was purchased from Strem Chemicals. Prior to use, the powders were calcined in a tube furnace at 400 °C overnight under air.

2.2 Calculation of cerium concentration and the number of Ce atoms per particle

Cerium concentration was determined using ICP-MS analysis. An aliquot (0.1 mL) of room temperature CeO_{2-x} NPs in DCM was dried under vacuum, and the sample was calcined at 400 ^oC for 4 hours to remove residual organic matter. After calcination, samples were digested in a 1 mL mixture of 1:1 concentrated H_2SO_4 and 50% aqueous H_2O_2, and diluted to a volume of 10 mL with DDW in a volumetric flask. Five samples were then prepared for ICP analysis and the concentration determined by the method of standard additions.

The average volume of each CeO_{2-x} NP and the number of Ce atoms/NP was calculated according to the procedure in the supporting information of Damatov et al. *Inorg. Chem.* **2018**. *57*, 14401.[6] For olea-Ce, oley-Ce, and uc-Ce, there are ca. 50, 650, and 2900 Ce atoms/NP.

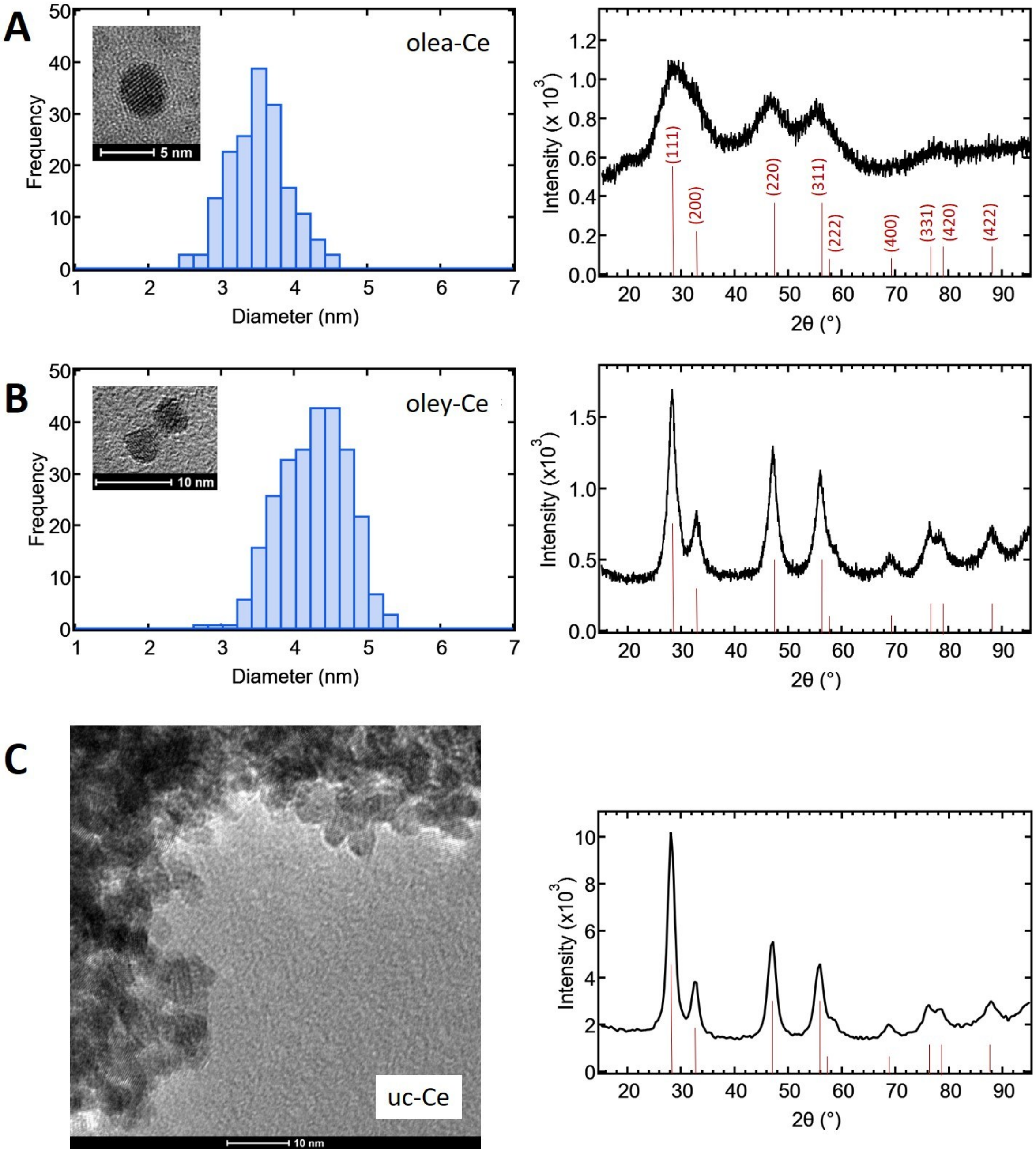

Figure SI-1. TEM and XRD of cerium oxide systems. XRD (scan rate of 0.1 deg/min) of A) oleate-capped ceria, B) oleylamine-capped ceria, and C) Strem ceria nanopowder are in accordance with standard data (red bars, JCPDS 34-0394). The breadth of the diffraction peaks in A, B and C reflect the average size of the nanocrystals according to the Scherrer formula, which gave average diameters of 1.6 ±1 nm, 3.9 ± 1 nm, and 6.2 ± 1 nm, respectively.

3 Catalyst considerations

3.1 Preparation of Ir and Ru catalysts

The iridium catalysts with pyridinesulfonamide ligands ([Ir-SO_2(R)], R = tol, Me, OMe) were received from the O'Connor group at The College of New Jersey.[7] Upon activation at moderate temperatures, these catalysts perform transfer hydrogenations in neat IPA at low catalyst loadings without base.[7,8] Observation of [Ir-SO_2(R)] hydride species were not reported.

The Noyori-Ikariya pre-catalyst RuCl(*p*-cymene)[(*S,S*)-Ts-DPEN] was obtained from Sigma Aldrich. The deprotonated and hydride forms of the catalyst were prepared according to a published procedure.[9] Briefly, the orange pre-catalyst was treated with KOH and water in dichloromethane at room temperature under N_2. The resulting purple organic layer was washed with water, dried over CaH_2, and concentrated to dryness under vacuum. The purple deprotonated complex [Ru] was stored in an N_2 glovebox at room temperature. To afford the hydride [RuH_2], the purple complex was dissolved in isopropanol, resulting in a red solution that affords a mixture of two enantiomers. The solvent was removed *in situ*, and the dark red solid was washed with cold pentane. A single enantiomer may be isolated as yellow crystals by recrystallization of the dark red solid in cold methanol as a concentrated solution. Heating overnight in organic solution leads to reappearance of the second enantiomer, causing the yellow color of the solution to become more orange-red. The UV-visible spectra of the deprotonated and the hydride forms, collected in toluene (0.37 mM), are shown below.

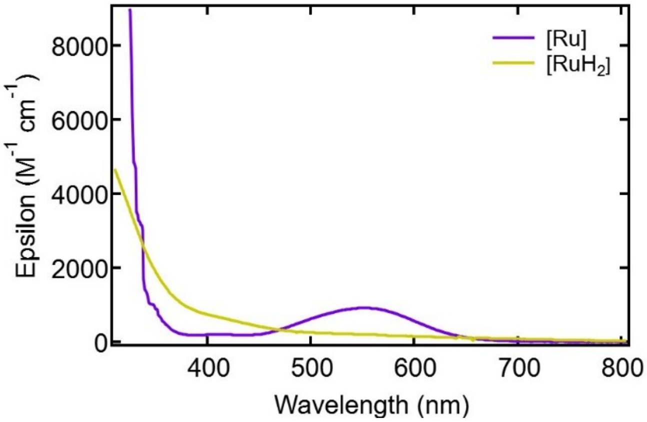

Figure SI-2. UV-visible spectra for [Ru] and [RuH_2]. The spectra for the [Ru] and [RuH_2] forms are distinct by UV-visible spectroscopy. An absorbance feature at about 550 nm is characteristic of the deprotonated ruthenium complex (purple).

4 Experiments with colloidal ceria and [RuH_2]

To confirm the observed reactivity between [RuH_2] and oley-Ce, the UV-visible spectra of each reagent alone was monitored under heating at 40 °C in toluene over several days. No conversion from [RuH_2] to [Ru] is observed from heating over several days. No reduction or shift in the band edge of oley-Ce is observed upon heating the NPs over several days.

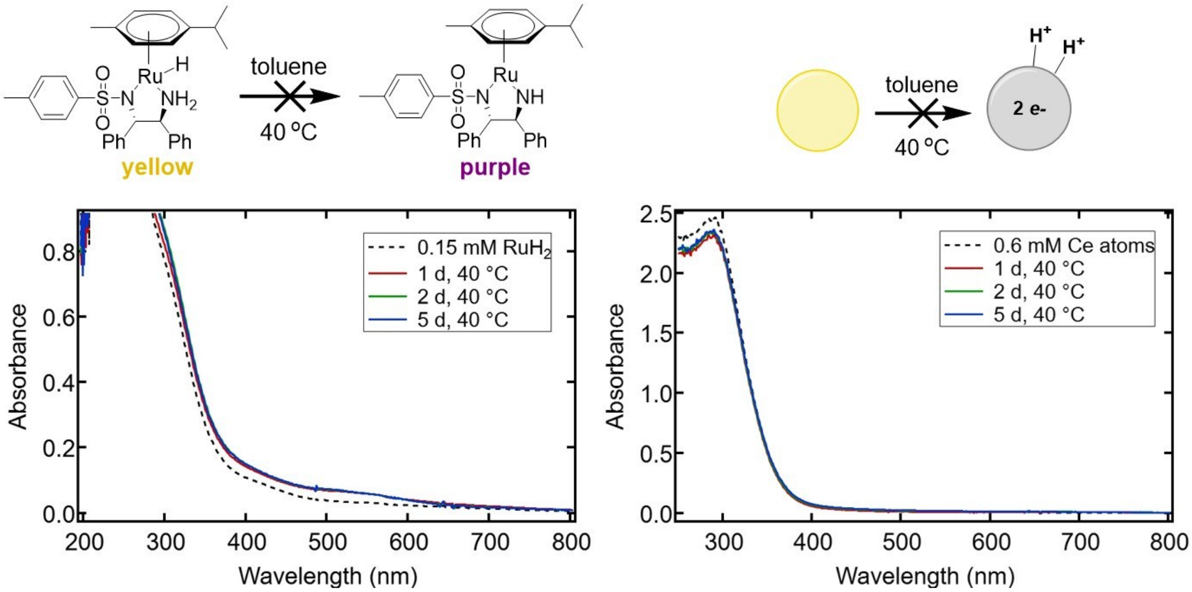

Figure SI-3. Heating controls of [RuH_2] or oley-Ce NPs. Toluene solutions containing only the Noyori hydride (left) or oley-Ce nanoparticles (right) are relatively stable under heating over several days as monitored by UV-visible spectroscopy

The spectra in Figure SI-4 are the complementary NMR experiment to the UV-visible and XAS studies described in the main manuscript (Results and Discussion, *Stoichiometric oxidation section*). The reaction of interest is shown below between oley-Ce and [RuH_2].

NMR spectra were collected in tol-d_8 over 24 hours. Residual solvent peaks (*) and the internal standard trimethoxybenzene (TMB) are labeled in gray. Selected regions are highlighted to show the proton signals that have little convolution from other signals. The highlighted regions, which correspond to the colored circles on the equation above the spectra, show protons from the hydride and *p*-cymene (2 methyl groups on the isopropyl moiety) group.

Several regions of the NMR spectra appear particularly convoluted due to overlapping signals resulting from (i) the [Ru] product, (ii) [RuH_2] and the reemergence of its other enantiomer, and (iii) oleylamine bound to oley-Ce. It is not unusual that ligands bound to NPs typically have broad peaks by NMR. A comparison of the experimental spectra with free (unbound) oleylamine ligand and independently collected [Ru] spectrum is also shown (gray).

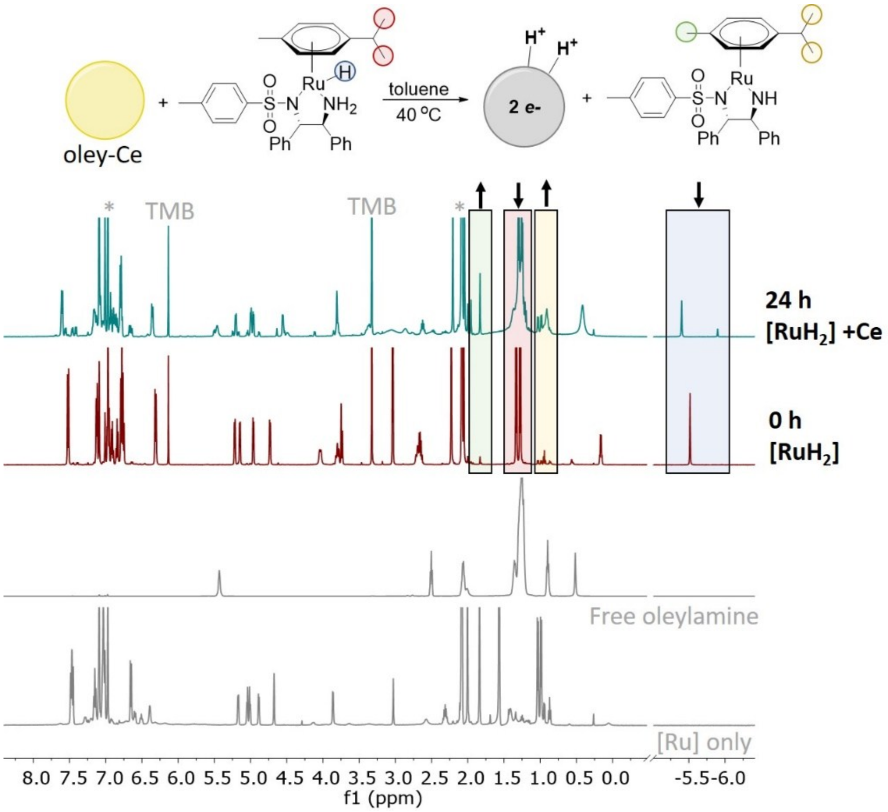

Figure SI-4. ^1H NMR of oley-Ce and [RuH_2]. Conversion of [RuH_2] to [Ru] in the presence of oley-Ce NPs over 24 hours after heating at 40 °C in toluene. The resulting 24 hours spectrum is convoluted by a mixture of species, but clearly shows several resonances (labeled to corresponding protons in the equation above by color) that indicated the disappearance of [RuH_2] (red and blue) and the appearance of [Ru] (green and yellow).

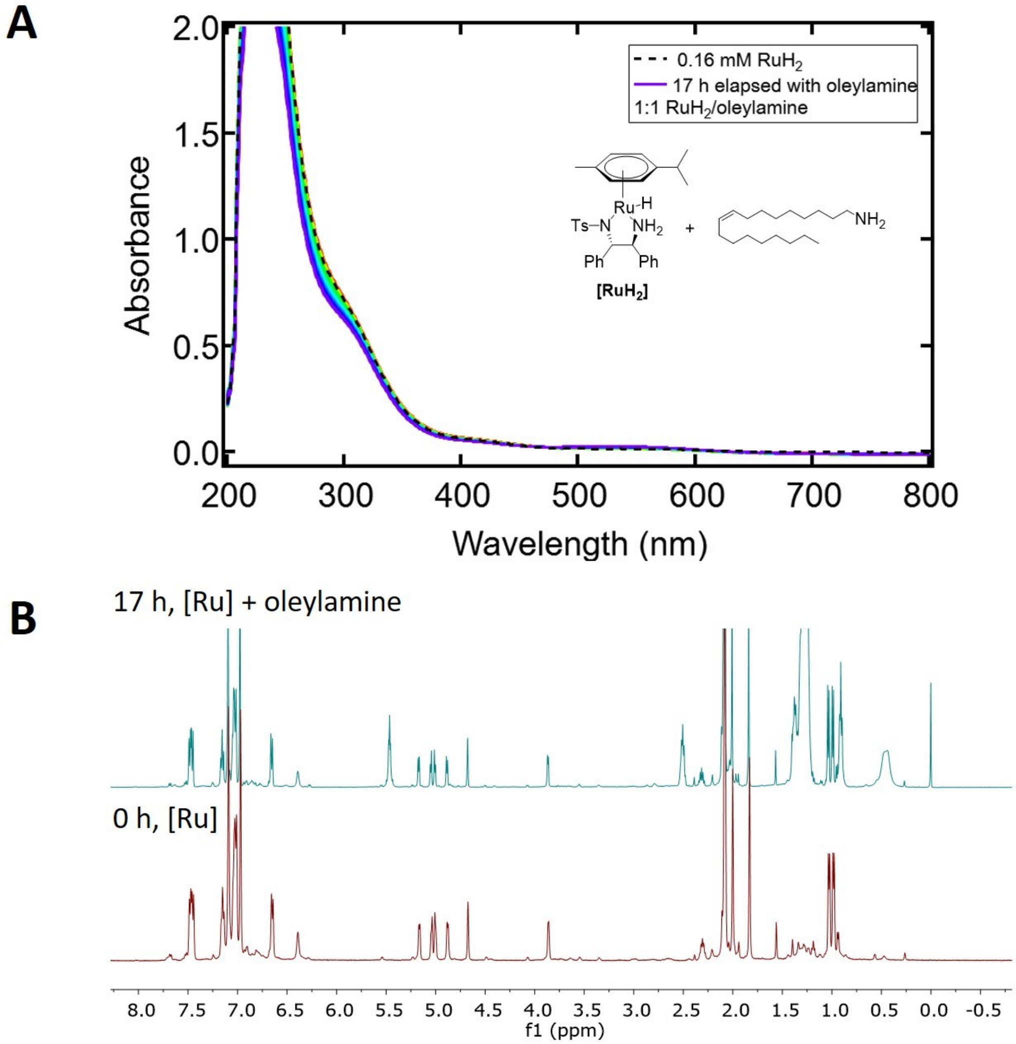

Figure SI-5. No effect of oleylamine capping ligand on [RuH$_2$]. A) Control reaction between [RuH$_2$] and oleylamine. There is little change by UV-visible spectroscopy and no visual indication that the solution has changed. B) Following the addition of oleylamine to a solution of [Ru] and heating at 40 °C, the ^{1}H NMR spectrum of [Ru] does not change other than appearance of peaks originating from free oleylamine.

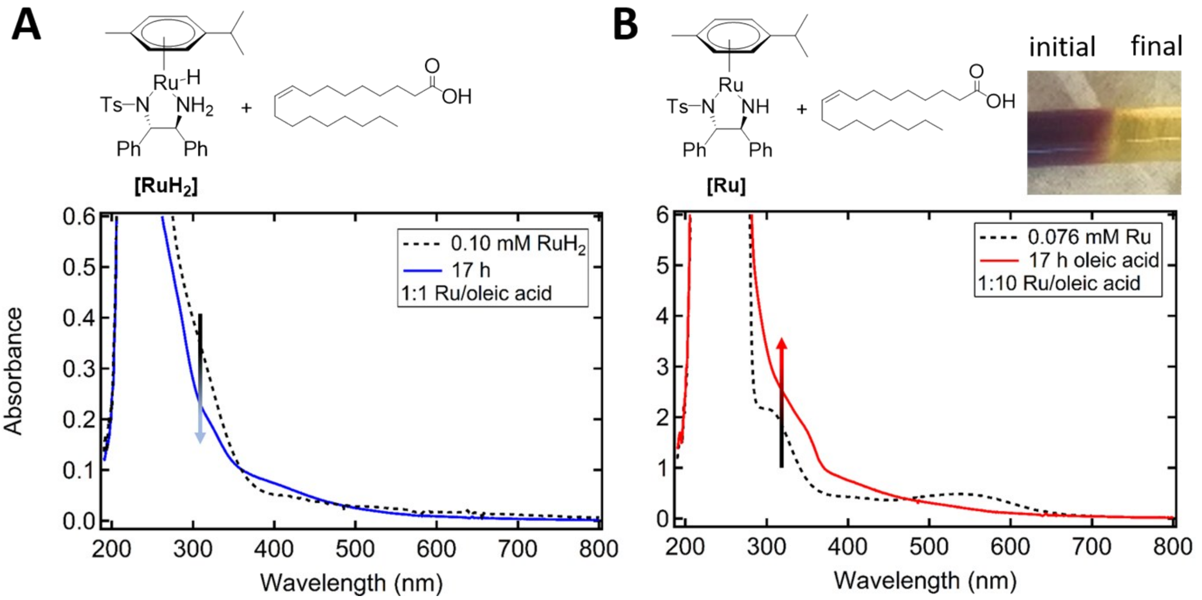

Figure SI-6. Effect of oleate capping ligand on [Ru] and [RuH_2]. Control reactions between A) [RuH_2] or B) [Ru] and oleic acid indicate both forms of the Noyori catalyst are reactive towards oleate. Instantaneous changes in the UV-visible spectra, also visible by eye, occur up addition of oleic acid.

4.1 Comments on the compatibility of capping ligands and homogeneous catalysts

In our survey of chemistry in this general area, the incompatibility between organically capped nanoparticles and reactive homogeneous catalysts has been a common problem. Analogous studies using Shvo's catalyst parallel those observed with the Noyori catalyst [Ru] – XAS and NMR methods indicated reduction of ceria and conversion of the hydride - although the results were convoluted by a competing reaction of the ligand and catalyst. Similarly, our laboratory's initial exploration of combining olea-Ce with the Goldman alkane dehydrogenation catalyst (PCP)IrH_n (PCP = κ^3-C_6H_3-2,6-[$CH_2P(t\text{-}Bu)_2$]$_2$ appeared to be derailed by formation of an iridium-oleate complex (by analogy with the known acetate derivative[10]).

5 ^{1}H NMR reactivity of uc-Ce and [RuH$_2$]

Similar to the study of colloidal oley-Ce with [RuH$_2$], uncapped cerium oxide (uc-Ce) was followed by UV-visible spectroscopy (*main text, Figure 2*) and ^{1}H NMR. The ^{1}H NMR time course is shown below. For the experiment, a mixture of 1:44 [RuH$_2$] : Ce atoms in deuterated toluene was sealed in a J-young NMR tube with a small stir bar under inert atmosphere. The reaction was heated with stirring at 40 °C. For each time point, the stir bar was removed in an N$_2$ glovebox, and the tube was centrifuged to collect the solid ceria at the bottom of the tube. Similar to the colloidal experiment, peaks are referenced relative to the internal standard TMB.

There is no complication of ligand signals anymore with the use of uc-Ce. However, there is still overlap between the [Ru] product, [RuH$_2$], and the reemergence of [RuH$_2$]'s enantiomer. Figure SI-7 A shows regions of interest in the NMR spectra, particularly the 2 equivalent methyl groups on the p-cymene ring and the hydride signals.

Corresponding conversion of [RuH$_2$] to [Ru] at the various time points from the NMR reaction is shown in part B of the figure. An image of the NMR tubes containing the reaction and its control is included just above the graph. Note that the reaction solution of [RuH$_2$] and uc-Ce changes color to purple (characteristic of [Ru]), and the uc-Ce at the bottom of the tube is gray in color (characteristic of reduced ceria).

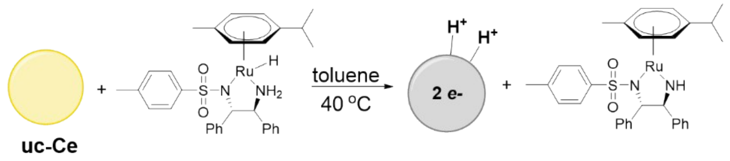

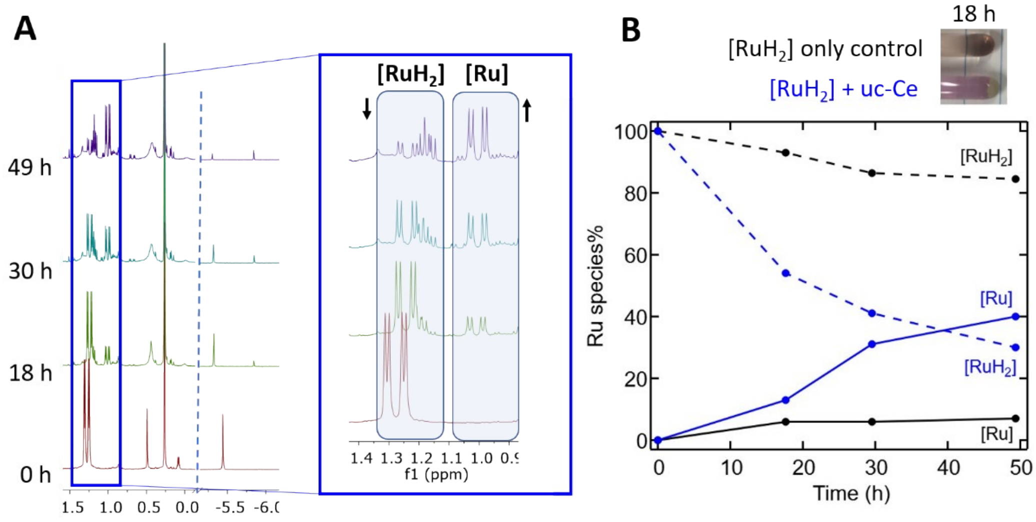

Figure SI-7. ^{1}H NMR of uc-Ce and [RuH$_2$]. A) Regions of interest in the ^{1}H NMR spectra of the [RuH$_2$] + uc-Ce reaction showing the growth of [Ru] peaks on the p-cymene ring and the decrease in the signal in the hydride region. B) The [RuH$_2$]% and [Ru]% as a function of time after heating at 40 °C are shown for the reaction of [RuH$_2$] + uc- Ce atoms (blue) and the control where no ceria is added (black). In the presence of ceria, some mass balance of Ru is lost.

6 Alcohol oxidation experiments

6.1 Screening of [Ir-SO_2(R)] catalysts for alcohol oxidation

To determine the optimal Ir analogue for use in alcohol oxidation studies, initial experiments with uc-Ce were conducted in neat isopropanol with various [Ir-SO_2(R)] complexes.

We hypothesized that use of the pure solvent as the reductant should push the reaction forward to form the (unobserved) iridium hydride, which would reduce the uc-Ce. Hence, [Ir-SO_2(R)], R = Me, Ph-OMe, tol, Ph-CN (0.10 mmoles) was added to a suspension of uc-Ce (0.35 mmoles Ce atoms) and the mixture was heated at 90 °C in neat IPA over 12 hours under inert atmosphere. The cerium nanopowder was separated from the reaction mixture and washed for analysis. The powder showed the characteristic visual color change to grayish purple and characteristic features for a reduced ceria spectrum using the CLARiTY spectrophotometer.

XAS of pressed pellets of the uc-Ce at the Ce-L_3 edge, obtained at the APS at Argonne National Lab, showed an increase in Ce^{3+}%. Analysis of the XANES spectra gave Ce^{3+}% values from 19% to 28%. The highest degree of Ce reduction resulting from the methyl-substituted iridium catalyst, so that derivative was chosen for the catalytic experiments. The native uc-Ce was found to contain 16% Ce^{3+}, and heating ceria in IPA without catalyst did not show reduction by XAS.

The XAS experiments determine the average cerium oxidation state throughout the material, and presumably it is primarily the ceria surface that is reactive. For the uc-Ce, a minimum of ca. 26% of ceria atoms are on the surface, so the observed increases in Ce^{3+}% observed by XAS are significant. The data indicate that the iridium complexes catalyze reduction of nanoceria by IPA.

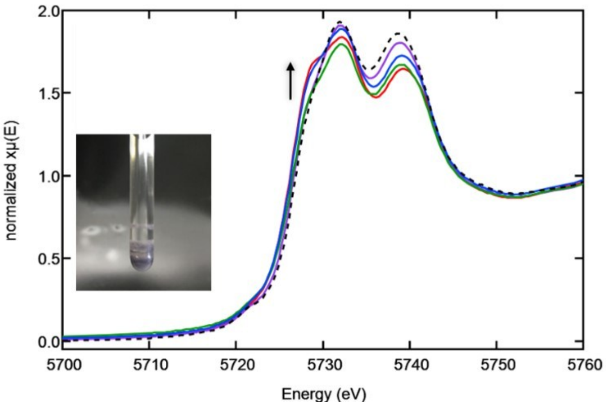

Catalyst	Ce(III) %
R = Me	28%
R = tol	25%
R = Ph-OMe	22%
R = Ph-CN	19%
Native	16%

Figure SI-8. XAS of uc-Ce reduced by various [Ir-SO2(R)] catalysts. CeO_{2-x} nanopowder were reduced using various substituted iridium catalysts [Ir-SO_2(R)] in neat isopropanol. The black arrow indicates the increase in Ce^{3+}%, a shoulder that appears near the edge energy of 5726 eV. A representative picture of the reduced, purple-gray ceria is shown in the image.

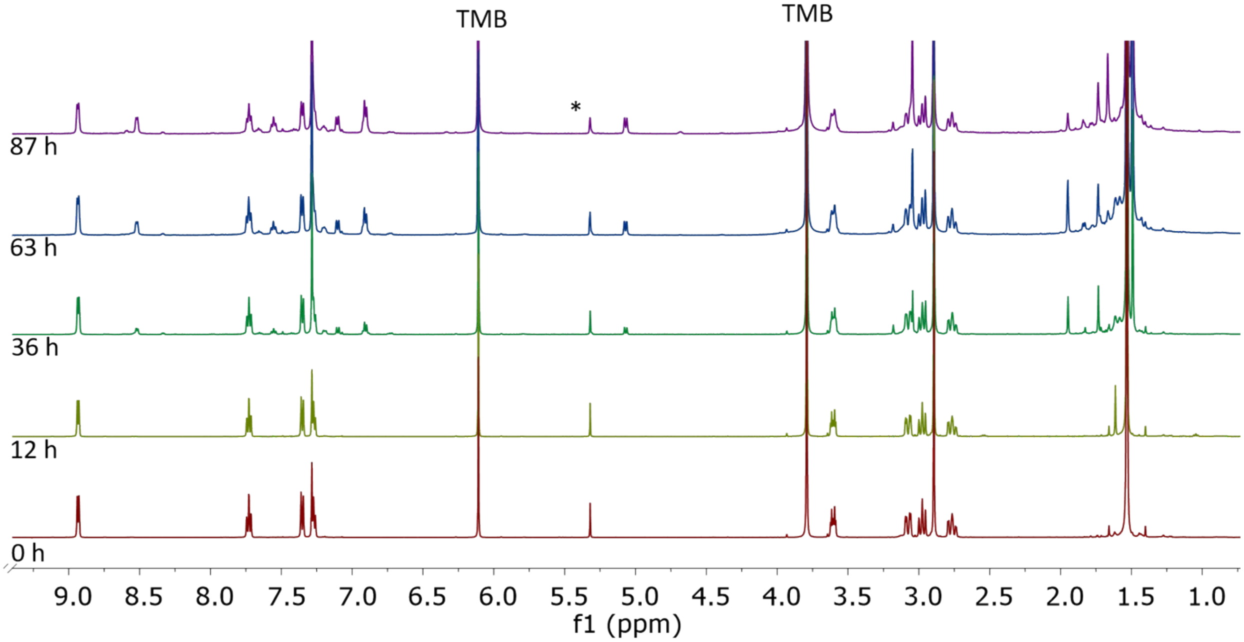

Figure SI-8. Heating of [Ir-SO_2(Me)] and uc-Ce. ^{1}H NMR of [Ir-SO_2(Me)] heated at 80 °C over 87 hours in the presence of uc-Ce in $CDCl_3$. Over the course of the control, the catalyst is relatively stable in the presence of ceria. After 36 hours, 90% of the catalyst remains, with new peaks corresponding to unbound ligand. At the end of the reaction, 80% of the catalyst was left in solution.

6.2 Experimental for catalytic alcohol oxidation reactions

In general, for each alcohol substrate, three reactions were conducted: catalyst + ROH (acceptorless), ROH + ceria, and catalyst + ROH + ceria. For reactions with all substrates, the reaction mixture contained [Ir-SO_2(Me)] : ROH : Ce atoms (of uncapped CeO_{2-x}, uc-Ce) in the stoichiometry of 0.55 : 100 : 800 in deuterated toluene. Each reaction solution was loaded into a J-Young NMR tube equipped with a flea stir bar. The sealed J-Young tubes were then heated in an oil bath 80 °C until there was little change in alcohol conversion, either 84 or 120 h.

To obtain spectra at various timepoints, the tubes were removed from the oil bath and their stir bars removed from the tube. For anaerobic reactions, this procedure was performed in an N_2 glovebox. For reactions under air, this was done under atmosphere to replenish any consumed oxygen. The tubes were then centrifuged to collect all ceria powder at the bottom of the tube to allow NMR to be taken of the homogeneous solution. After collecting spectra, the stir bar was re-added to the J-Young tube either in the glovebox or under air. The tube was shaken and sonicated to re-suspend the uc-Ce.

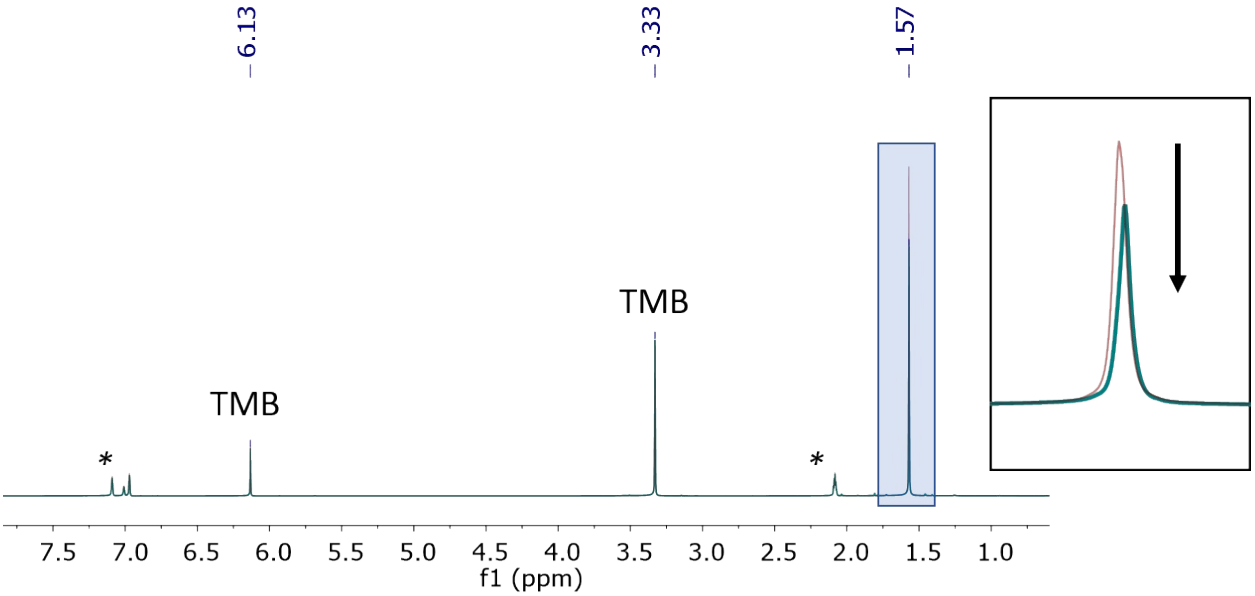

Figure SI-9. Adsorption of acetone to uncapped cerium oxide. Heating overnight of a 77 mM solution of acetone in toluene-d_8 at 90 °C in the presence of uc-Ce (1:1 Ce atoms/acetone) resulted in a decrease of the acetone signal by 28%.

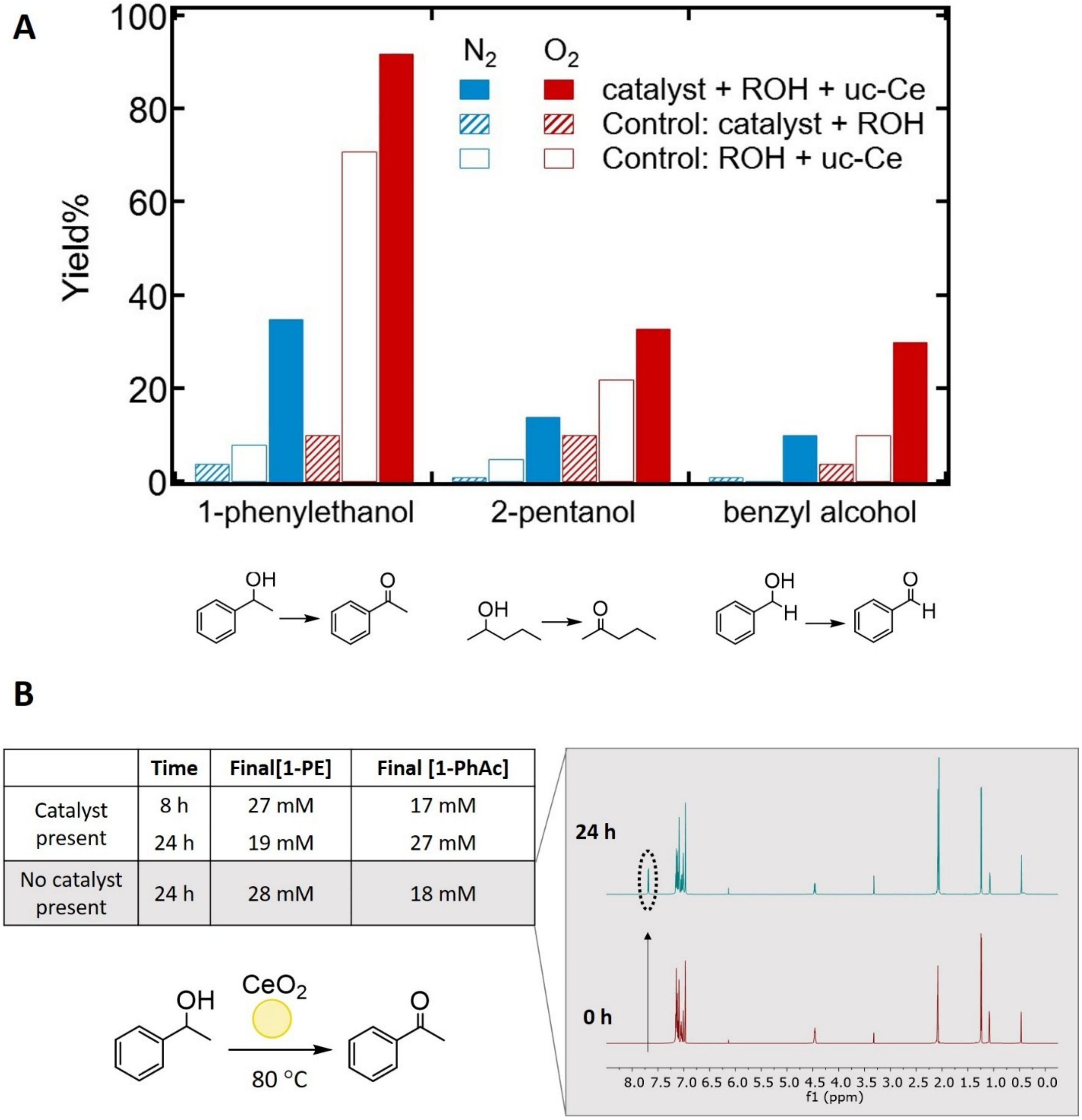

	Time	Final[1-PE]	Final [1-PhAc]
Catalyst present	8 h	27 mM	17 mM
	24 h	19 mM	27 mM
No catalyst present	24 h	28 mM	18 mM

Figure SI-10. Aerobic oxidation of substrates. A) The yields of product from two controls and the 3-component catalytic system heated at 80 ° C over five days are shown under anaerobic (blue, depicted in Figure 5) and aerobic (red) conditions where [Ir-SO_2(Me)] : ROH : Ce atoms 0.55 : 100 : 800. The two controls include reaction of only the catalyst with alcohol (stripes), and the reaction of only ceria and alcohol (dots). In comparison to the anaerobic reactions, the aerobic reactions show greater yield of the oxidation product due to the ability of ceria to oxidize in air. B) In examining the case of 1-PE more closely, when no catalyst is present, some 1-phenylethanone [1-PhAc] is produced. However, more [1-PhAc] is produced when the Ir catalyst is included. After 24 hours, the catalyst system yields 27 mM [1-PhAc], while the no catalyst system yields only 18 mM [1-PhAc] (achieved by the catalyst containing system in only 8 hours).

7 Reaction of cerium oxide and dihydroanthracene

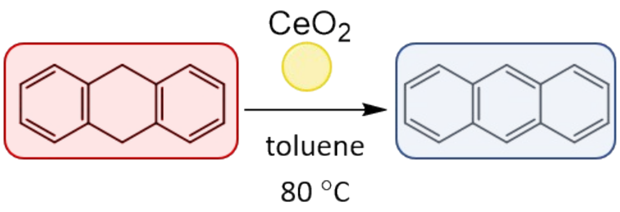

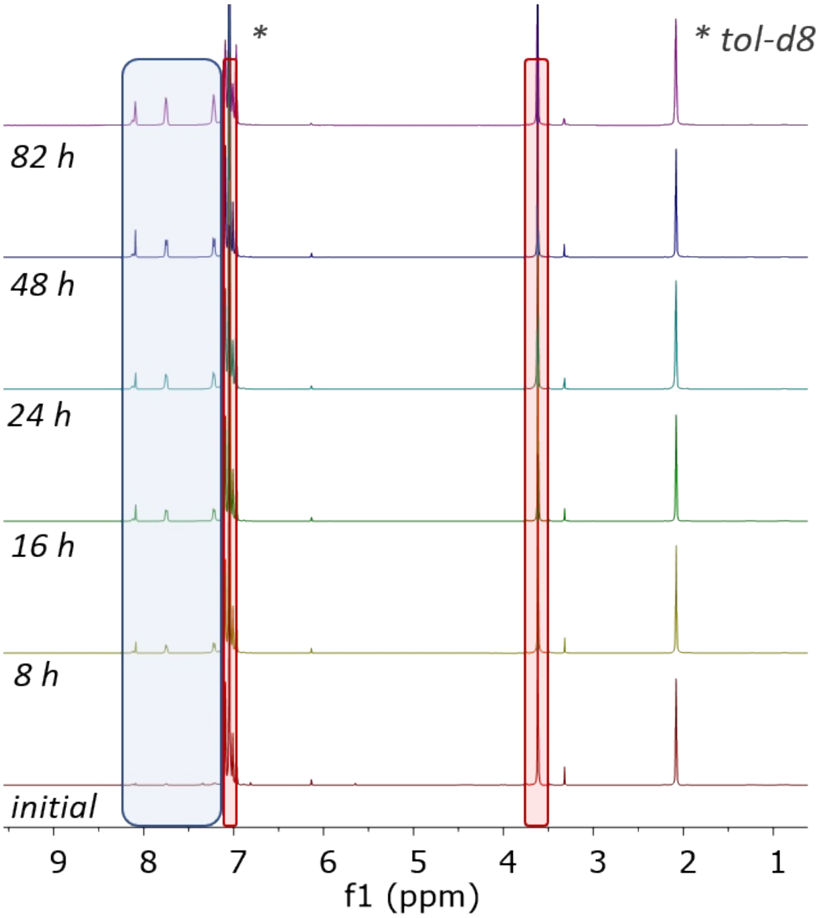

Figure SI-11. Reaction of uncapped cerium oxide with dihydroanthracene. In a reaction between uc-Ce and DHA (red) under air, the primary product formed is anthracene (blue). A peak for an oxygen inserted product, anthraquinone, appears, but makes up only 3% of the reaction mixture.

8 Analysis of the size of cerium oxide post-reaction

By XRD and TEM, the size of the uncapped ceria (uc-Ce) is stable following the reaction with either [RuH_2] at 40 °C or alcohol + [Ir-SO_2(Me)] at 80 °C., and then oxidation under air Three samples were monitored:

1) uc-Ce + [RuH_2] (48 hours)
2) uc-Ce + 1-phenylethanol + [Ir-SO_2(Me)], inert atmosphere (84 hours)
3) uc-Ce + 1-phenylethanol + [Ir-SO_2(Me)], cycled with air every 12 hours (84 hours)

Similar to previous treatments described here, the uc-Ce was washed with ethanol post reaction to remove residual catalyst and separated from solution. The ceria was allowed to oxidize in air for several hours. XRD spectra were collected after drop casting the uc-Ce on a glass slide for measurement. The scan rate was 1 deg/min for all three samples. The average size of the native, untreated uc-Ce according to the Scherrer formula was calculated to be 6.2 ± 1 nm. The samples here calculate to be 5.2 ±1 nm (1, blue), 5.3 ± 1 nm (2, green), and 5.3 ± 1 nm (3, red). These values are in agreement within error and demonstrate the size is stable to the mild reaction conditions. These XRD spectra are shown below in Figure SI-12. The corresponding TEM spectra are shown in Figure SI-13, and show the spherical crystallite morphology is preserved.

A stability study of the colloidal oleate capped CeO_{2-x} was performed in a previous paper by TEM, in which the size of the NPs was monitored by TEM following reduction by 1,4-hydroquinone and oxidation by air. We found that mild chemical reactions did not significantly change the size of the NPs, and expect that to be true for the colloids in this study. The average diameters and widths of distributions were within error: 1.9 ± 0.2 nm (as prepared, native), 1.9 ± 0.2 nm (reduced by 1,4-hydroquinone), and 2.0 ± 0.3 nm (oxidized by air). The TEM images and size distributions of oleate capped ceria NPs at various redox states can be found in Figure S17 of D. Damatov, S. M. Laga, E. A. Mader, J. Peng, R. G. Agarwal, and J. M. Mayer, *Inorg. Chem.*, **2018**, 57, 22, 14401.

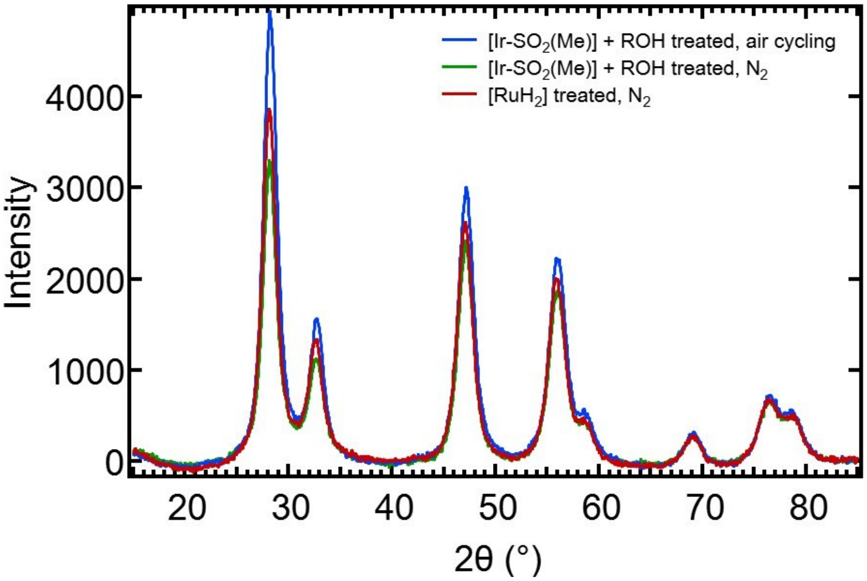

Figure SI-12. Post-reaction XRD spectra of uncapped cerium oxide. Overlayed XRD spectra of uc-Ce that was first chemically reduced and then oxidized in air. The uc-Ce was chemically reduced in three treatments: A) [RuH$_2$] under inert atmosphere for 48 hours (40 °C), B) [Ir-SO$_2$(Me)] + 1-phenylethanol under inert atmosphere for 84 hours (80 °C), C) [Ir-SO$_2$(Me)] + 1-phenylethanol cycled with air every 12 hours for 84 hours (80 °C). All spectra were measured at a scan rate of 1 deg/min. The average size according to the Scherrer formula was calculated to be 5.2 ±1 nm (blue), 5.3 ± 1 nm (green), and 5.3 ± 1 nm (red), respectively.

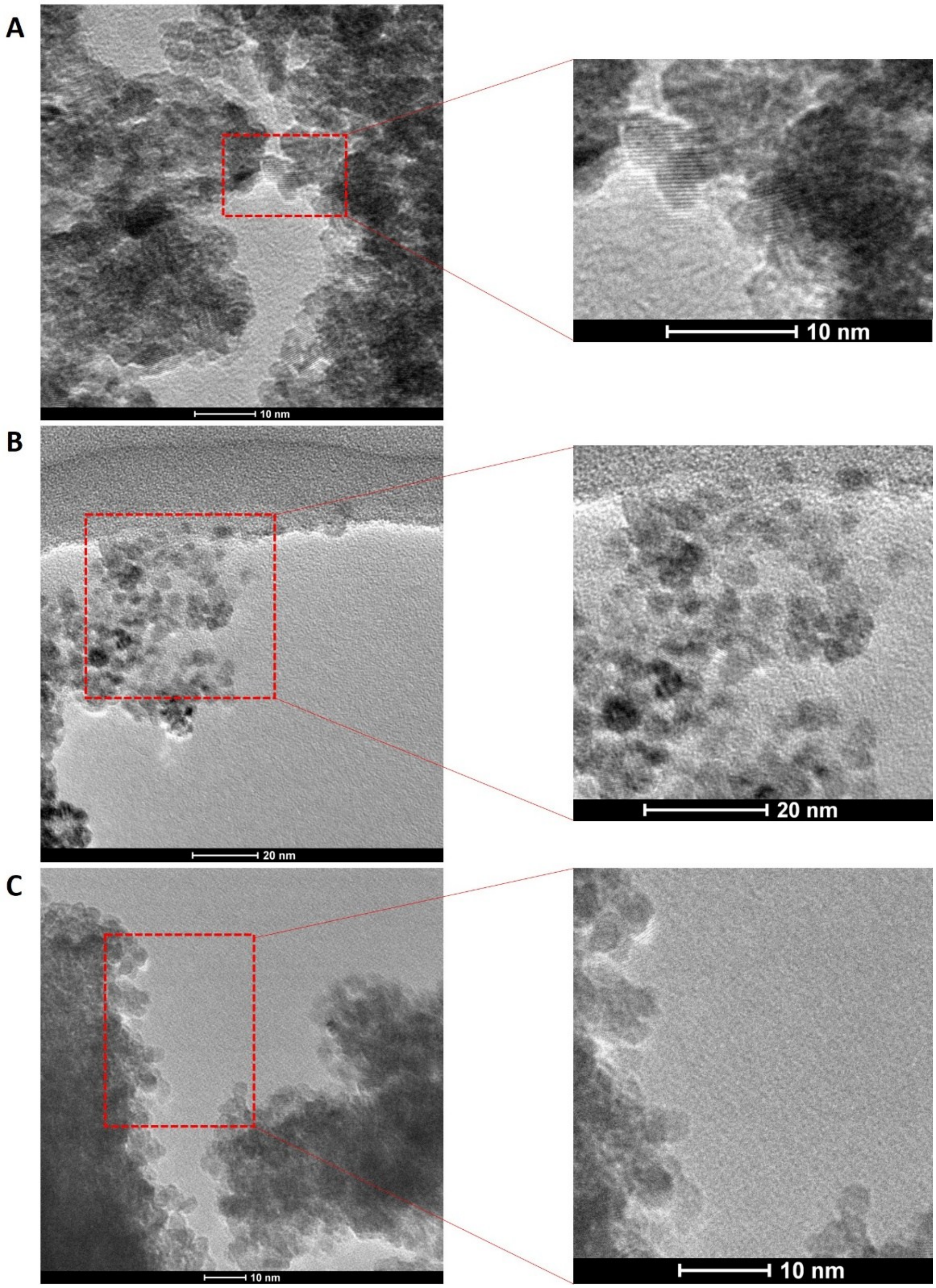

Figure SI-13. Post reaction TEM spectra of uncapped cerium oxide. TEM spectra of uc-Ce isolated from various reduction reactions, followed by oxidation in air. Prior to TEM, the uc-Ce was chemically reduced in three treatments: A) [RuH_2] under inert atmosphere for 48 hours (40 °C), B) [Ir-SO_2(Me)] + 1-phenylethanol under inert atmosphere for 84 hours (80 °C), C) [Ir-SO_2(Me)] + 1-phenylethanol cycled with air every 12 hours for 84 hours (80 °C). Various regions are highlighted to the right to better show the morphology and crystallinity of the uc-Ce.

9 References

1 P. Nachimuthu, W.-C. Shih, R.-S. Liu, L.-Y. Jang and J.-M. Chen, The Study of Nanocrystalline Cerium Oxide by X-Ray Absorption Spectroscopy, *J. Solid State Chem.*, 2000, **149**, 408–413.

2 F. Zhang, P. Wang, J. Koberstein, S. Khalid and S.-W. Chan, Cerium oxidation state in ceria nanoparticles studied with X-ray photoelectron spectroscopy and absorption near edge spectroscopy, *Surf. Sci.*, 2004, **563**, 74–82.

3 Clarity Spectrophotometers | OLIS, Inc. | United States, https://www.olisclarity.com/, (accessed November 2019).

4 T. Taniguchi, T. Watanabe, N. Sakamoto, N. Matsushita and M. Yoshimura, Aqueous Route to Size-Controlled and Doped Organophilic Ceria Nanocrystals, *Cryst. Growth Des.*, 2008, **8**, 3725–3730.

5 T. Yu, J. Joo, Y. I. Park and T. Hyeon, Large-Scale Nonhydrolytic Sol–Gel Synthesis of Uniform-Sized Ceria Nanocrystals with Spherical, Wire, and Tadpole Shapes, *Angew. Chem. Int. Ed.*, 2005, **44**, 7411–7414.

6 D. Damatov, S. M. Laga, E. A. Mader, J. Peng, R. G. Agarwal and J. M. Mayer, Redox Reactivity of Colloidal Nanoceria and Use of Optical Spectra as an In Situ Monitor of Ce Oxidation States, *Inorg. Chem.*, 2018, **57**, 14401–14408.

7 A. Ruff, C. Kirby, B. C. Chan and A. R. O'Connor, Base-Free Transfer Hydrogenation of Ketones Using Cp*Ir(pyridinesulfonamide)Cl Precatalysts, *Organometallics*, 2016, **35**, 327–335.

8 T. M. Townsend, C. Kirby, A. Ruff and A. R. O'Connor, Transfer hydrogenation of aromatic and linear aldehydes catalyzed using Cp*Ir(pyridinesulfonamide)Cl complexes under base-free conditions, *J. Organomet. Chem.*, 2017, **843**, 7–13.

9 K.-J. Haack, S. Hashiguchi, A. Fujii, T. Ikariya and R. Noyori, The Catalyst Precursor, Catalyst, and Intermediate in the RuII-Promoted Asymmetric Hydrogen Transfer between Alcohols and Ketones, *Angew. Chem. Int. Ed. Engl.*, 1997, **36**, 285–288.

10 S. Kundu, J. Choi, D. Y. Wang, Y. Choliy, T. J. Emge, K. Krogh-Jespersen and A. S. Goldman, Cleavage of Ether, Ester, and Tosylate C(sp3)–O Bonds by an Iridium Complex, Initiated by Oxidative Addition of C–H Bonds. Experimental and Computational Studies, *J. Am. Chem. Soc.*, 2013, **135**, 5127–5143.